

H I absorption in high-frequency peaker galaxies

M. Orienti^{1,2}, R. Morganti^{3,4}, and D. Dallacasa^{1,2}

¹ Dipartimento di Astronomia, Università di Bologna, via Ranzani 1, 40127 Bologna, Italy
e-mail: orienti@ira.inaf.it

² Istituto di Radioastronomia – INAF, via Gobetti 101, 40129 Bologna, Italy

³ Netherlands Foundations for Research in Astronomy, Postbus 2, 7990 AA Dwingeloo, The Netherlands

⁴ Kapteyn Astronomical Institute, University of Groningen, PO Box 800, 9700 AV Groningen, The Netherlands

Received 5 January 2006 / Accepted 4 July 2006

ABSTRACT

WSRT observations have been used to investigate the presence of neutral hydrogen in extremely young radio galaxies. These objects were selected from a sample of High-Frequency Peakers (HFPs). We detect 2 of the 6 observed galaxies confirming previous detection of H I in these objects. In the case of OQ 208 – for which discrepant results were available – we confirm the presence of a broad ($\sim 1800 \text{ km s}^{-1}$), blue-shifted and shallow H I absorption. No significant changes in the H I profile have been found between the two epochs of the observations. The intriguing result is that the derived H I column densities and upper limits obtained for the most compact sources, do not follow the inverse correlation between the column density and the linear size found for CSS/GPS sources. This can be explained – assuming the gas is already in a torus/disk structure – by a combination of the orientation and the extreme compactness of the sources. In this scenario, our line of sight to the source would intersect the torus in its inner region with low optical depth due to high spin and kinetic temperatures. There is no evidence, with the exception of OQ 208, of unsettled, high column density gas still enshrouding the young radio sources. This can be due to the low filling factor of such a medium.

Key words. galaxies: active – galaxies: evolution – radio continuum: galaxies – radio lines: galaxies

1. Introduction

A substantial amount of gas and dust is often found in the central regions of galaxies harbouring an Active Galactic Nucleus (AGN). This gas provides important information on the physical conditions and processes in these near-nuclear regions (Morganti et al. 2004a; Peck et al. 1999). A component of this gas, the atomic hydrogen, can be studied in radio-loud objects via absorption detected against the strong continuum source. Since years, a large number of detailed studies has been done (see e.g. Heckman et al. 1983; van Gorkom et al. 1989; Morganti et al. 2001, 2004a, 2005; Vermeulen et al. 2003; Pihlström et al. 2003) and they have shown that the neutral hydrogen can be associated with different structures, from circumnuclear tori to fast outflows. These results have been crucial for constructing our present picture of the nuclear structure of radio loud AGN.

The medium enshrouding the nuclear regions also plays an important role in the growth and evolution of the radio source (Labiano et al. 2006). The presence of significant amount of gas in young radio galaxies is supported by a larger incidence of H I absorption in these objects (Vermeulen et al. 2003; Pihlström et al. 2003) compared to what typically found in old and larger radio sources (van Gorkom et al. 1989; Morganti et al. 2001). This dense medium is likely the result of the merger that triggered the radio source (Morganti et al. 2004b). Thus, in the initial phase of the radio source, the radio jet likely has to make its way through a relatively dense medium that surrounds the active nucleus.

The radio galaxies classified as “Compact-Steep Spectrum” and “GHz-Peaked Spectrum” are believed to represent the early stages of the radio activity (Fanti et al. 1995; Readhead et al. 1996; Snellen et al. 2000). These radio sources are intrinsically

small (sub-galactic size, i.e. $< 15 \text{ kpc}$) and bright ($P_{1.4 \text{ GHz}} > 10^{25} \text{ W/Hz}$), characterised by a convex radio spectrum, peaking at frequencies between 100 MHz and a few GHz. Their radio morphologies appear to be the scaled-down version of powerful edge-brightened radio galaxies, with luminous mini-lobes (~ 0.1 up to few kpc) and weaker jets and cores. Both kinematic (Polatidis & Conway 2003), and spectral (Murgia 2003) studies strongly support the youth scenario, indicating ages of 10^3 – 10^5 years.

Given the relatively high detection rate of H I absorption in these objects (Vermeulen et al. 2003; Pihlström et al. 2003), it is of particular interest to investigate the characteristics of the nuclear interstellar medium (ISM) in even younger radio sources. In the youth scenario, the anti-correlation between the turnover frequency and the linear size (O’Dea 1998), which is indicative of the age, suggests that the youngest sources have the highest turnover frequency. Therefore, the “High-Frequency Peaker” (HFP) radio sources, characterised by the same properties of CSS/GPS, but with the spectral turnover occurring at frequencies higher than 5 GHz, are good candidates to be *newly born* radio sources, with ages of about 10^2 – 10^3 years (Dallacasa 2003).

This paper reports on the result of observations searching for H I absorption in a sample of 6 HFP radio sources, selected from the Dallacasa et al. (2000) bright HFP sample, and suitable to be observed at the Westerbork Synthesis Radio Telescope (WSRT).

2. The sample

The bright HFP sample (Dallacasa et al. 2000) has been constructed by cross-correlating the Green Bank Survey (87GB) at 4.9 GHz and the NRAO VLA Sky Survey (NVSS) at 1.4 GHz. Only the sources with a flux density brighter than 300 mJy at

4.9 GHz and with a rising spectrum steeper than $\alpha = -0.5$ ($S \propto \nu^{-\alpha}$; i.e. to avoid turnover frequencies ≤ 5 GHz) have been selected as HFP candidates. To tackle the contamination of variable sources, like blazars, all the candidates have been simultaneously observed with the VLA at eight different frequencies from 1.4 to 22 GHz. The final sample consists of 55 sources ($\sim 3\%$ of the sources exceeding 300 mJy in the 87GB): 11 galaxies with redshifts ranging from 0.02 to 0.67; 33 quasars with higher redshifts, typically between 0.9 and 3.5; 5 BL Lac objects, while 6 sources still lack optical identification (Dallacasa et al. 2002; Dallacasa et al., in preparation). Since the selection of these sources is based on their simultaneous radio spectra at a single epoch, there is still some contamination by beamed radio sources, whose emission is temporarily dominated by a self-absorbed jet component. Further multi-frequency VLA observations to exclude the long-term variability (Tinti et al. 2005) and pc-scale resolution morphological analysis (Orienti et al. 2006), have been carried out to confirm genuine and young HFPs.

As shown by Orienti et al. (2006), there is a clear segregation in radio morphology between galaxies and quasars. The majority of galaxies (9/11) show a Compact-Symmetric-Object(CSO)-like morphology, while 28/33 quasars display “Core-Jet” or unresolved structures. This is consistent with the idea that the HFP spectrum in galaxies and quasars originates in different regions: mini-lobes and/or hot-spots in galaxies, compact regions related to the core and the jet base in quasars, in agreement with what found in GPS (Stanghellini et al. 2005) and bright CSS samples (Dallacasa et al. 1995; Fanti et al. 1990).

Since the radio sources hosted in galaxies likely represent a population of young radio sources, six out of the eleven HFP galaxies, have been observed to search for HI absorption. The selected objects have recessional velocities such that the redshifted HI line is shifted to frequencies that are known to be relatively free of radio interference (RFI) at the WSRT. Their redshift ranges from 0.02 and 0.67, and the flux densities at 1.4 GHz exceed 90 mJy.

For one of the five remaining HFP galaxies, WSRT observations were precluded, since a well known RFI (GSM) affects the frequency band, while for the other four sources, the optical redshift is not available.

3. WSRT observations and data reduction

The WSRT observations have been carried out in different runs from 29 January to 12 September 2005 in dual orthogonal polarisation mode. Two sources in the sample were already known to have HI absorption: from Carilli et al. (1998) in the case of J0111+3906 and Vermeulen et al. (2003) and Morganti et al. (2005) in the case of OQ 208. In these two sources, the goal of the new observations was to investigate the possible presence of variability in the HI absorption and/or a broad component in their absorption spectrum. In particular, in the case of OQ 208, the two previous observations report different characteristics (i.e. width) of the absorption.

Of the six observed galaxies, those with $z < 0.3$ have been observed for 6 h each, using the L-band receiver, with 1024 spectral channels covering a 20 MHz wide observing band. The sources with redshift higher than 0.4 have been observed for 12 h each, using the UHF-high band, with 1024 spectral channels. The 20 MHz band, allowed to cover a velocity range around the velocity centroid of approximately ± 2200 km s $^{-1}$ at $z = 0.07$, and approximately ± 3500 km s $^{-1}$ at $z = 0.6$. Only the source J0003+2129 has been observed with a 10 MHz wide band ($\sim \pm 1500$ km s $^{-1}$), since known RFI would have affected a

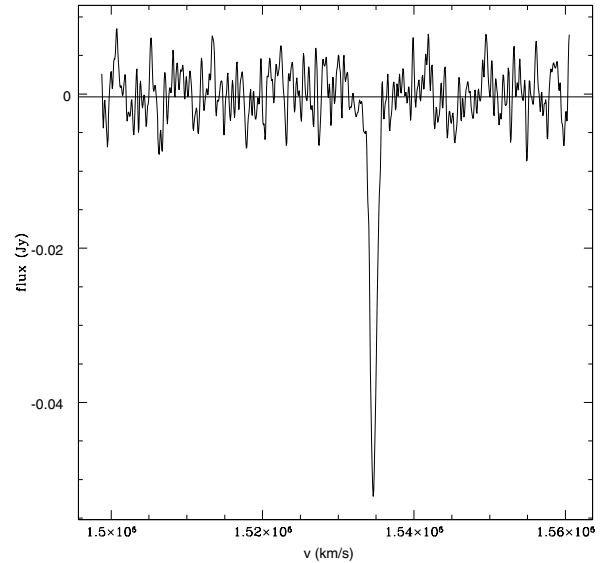


Fig. 1. The HI absorption profile detected in J0111+3906. The velocity is in the optical heliocentric convention.

wider band. Table 1 summarizes the observational and physical parameters of the sources.

The data reduction was carried out using the MIRIAD package. The quasars 3C 286, 3C 48 and 3C 147 were observed to calibrate the absolute flux density scale and the bandpass. Data were inspected for time-limited and baseline specific interference, and bad data were removed before solving for the gain- and band-pass calibrations. The two orthogonal linear polarisations were added together to improve the signal-to-noise ratio of the final spectrum. The continuum subtraction was done by using a linear fit through the line-free channels (i.e. all the channels outside a range of ± 1000 km s $^{-1}$ from the centroid frequency) of each visibility record and subtracting this fit from all the frequency channels (using the MIRIAD task “UVLIN”). Particular attention has been given to the case of OQ 208 where shallow absorption has been detected (see below). After several trials, the final continuum subtraction was obtained using as line-free those channels outside the range $-1700/+600$ from the centroid frequency. The baselines of the spectra obtained after the continuum subtraction result flat, indicating that no broad and shallow line features have been included.

After the continuum subtraction, line cubes were produced using uniform weighting, Hanning smoothed and inspected. For the two sources where HI absorption was detected (J0111+3906 and OQ 208), the spectra obtained at the location of the peak of the radio continuum are shown in Figs. 1 and 2. For every source, the rms noise was estimated from the line cube and the values are given in Table 1.

In order to make a reliable comparison between our values and what found in CSS/GPS samples, the upper limits to the optical depth and the HI column density have been computed following Vermeulen et al. (2003), i.e. assuming the 2σ noise level, a line width of 100 km s $^{-1}$ and T_{spin} of 100 K (see Table 1).

Finally, we have used the line-free channels to produce a continuum image of each target. The continuum emission is always unresolved at the resolution of the WSRT (typically about $20''$), with the only exception of J0111+3906, known to possess a relatively weak component on such angular scale (Baum et al. 1990). The continuum emission derived from our data is slightly resolved to the East, consistent with the large-scale emission seen by Baum et al. (1990).

Table 1. Physical and observational parameters of the 6 HFP galaxies observed with WSRT. Columns 1, 2: source names; Col. 3: projected linear sizes (Orienti et al. 2006); Col. 4: optical redshift; Col. 5: central frequency; Col. 6: channel resolution; Col. 7: 1σ noise level in the line cube; Col. 8: continuum flux density taken from our WSRT data at the observed frequency; Col. 9: peak flux density of the absorption line, measured on the spectral image; Col. 10: optical depth; Col. 11: the width of the HI absorption line: for J0111+3906 the *FWHM* is given, in the case of OQ 208 we give the *FWZI*, due to the complexity of the line profile; Col. 12: HI column density derived from $N_{\text{HI}} = 1.82 \times 10^{18} T_{\text{spin}} \tau_{\text{peak}} \Delta V \text{ cm}^{-2}$, a T_{spin} of 100 K has been assumed; Col. 13: the redshift of the peak HI absorption. The line flux density, the optical depth and the HI column density upper limits have been computed assuming the 2σ noise level, a line width of 100 km s^{-1} and T_{spin} of 100 K, as in Vermeulen et al. (2003). *a*: For the source J0111+3906, the projected linear size is taken from Owsianik et al. (1998).

Source J2000 (1)	Other name (2)	LS pc (3)	z_{opt} (4)	ν_{obs} MHz (5)	Resol. km s^{-1} (6)	rms mJy/b/ch (7)	S_{obs} mJy (8)	S_{HI} mJy (9)	τ_{peak} (10)	Δv km s^{-1} (11)	$\text{Log}(N_{\text{HI}})$ (12)	$z_{\text{HI,peak}}$ (13)
J0003+2129		22	0.452	977.96	4.3	6.1	50	<12.2	<0.15		<21.43	
J0111+3906	OC 314	22 ^a	0.668	851.32	6.9	2.8	170	52.7	0.44	100	21.90	0.6687
J0655+4100		<1	0.02156	1390.03	4.3	0.7	239	<1.4	<0.006		<20.0	
J1407+2827	OQ 208	10	0.0773	1318.60	4.5	1.1	826	5	0.005	1800	20.9	0.0769
J1511+0518		7	0.084	1309.96	9.5	1.1	80	<2.2	<0.02		<20.6	
J1623+6624		<1	0.203	1180.38	4.5	0.7	129	<1.4	<0.01		<20.3	

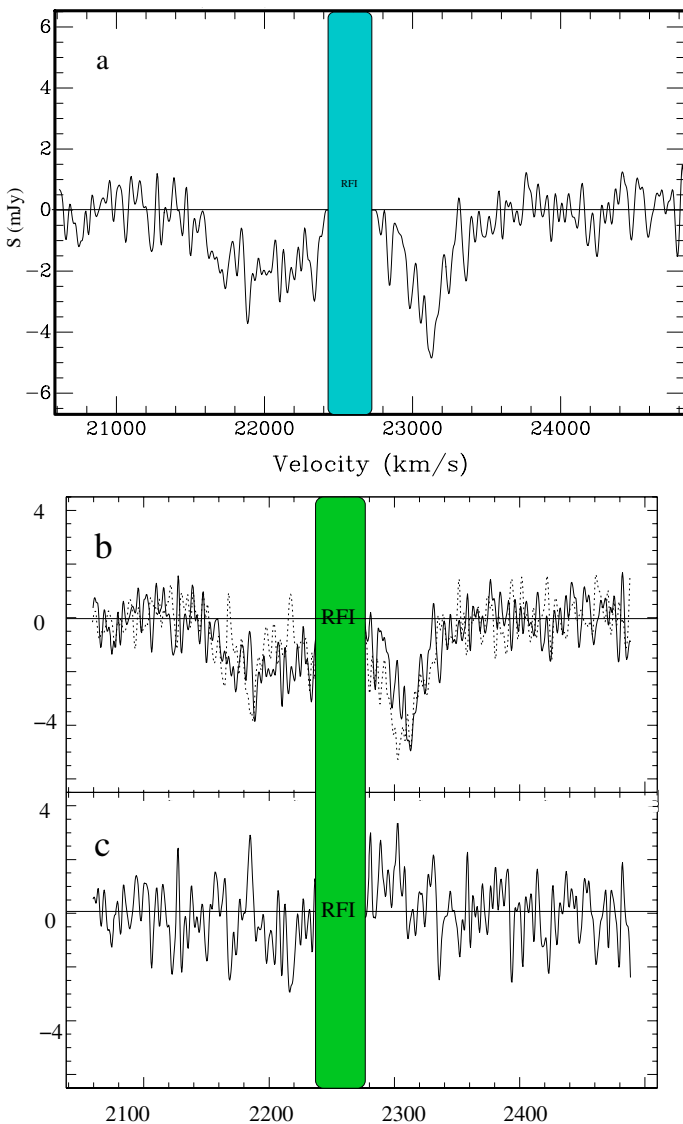


Fig. 2. **a)** The HI absorption profile detected in OQ 208 from our new WSRT observations. The velocity is in the optical heliocentric convention. Strong RFI is present in the line profile. **b)** The two-epoch line profiles of OQ 208 one superimposed to the other; the continuous line represents data from Morganti et al. (2005), while the dotted line represents our new data. **c)** The residuals obtained after subtracting the two-epoch line profiles.

4. Results

Of the six galaxies observed, we detect HI absorption only in the two sources (J0111+3906 and OQ 208) in which the presence of absorption was already reported by previous studies. In addition to this, we find HI in emission in two companion galaxies of J0655+4100. We discuss below these three objects in more detail.

4.1. The source J0111+3906

The radio source J0111+3906 is associated with a narrow emission line galaxy at $z = 0.668$ (Carilli et al. 1998). The source is classified as a Compact Symmetric Object (CSO), due to its VLBI-scale morphology (Taylor et al. 1996), but it also shows an extended emission on the kpc-scale, interpreted in terms of recurrency of the radio activity (Baum et al. 1990).

HI absorption was already reported by Carilli et al. (1998), based on narrow-band WSRT observations. We detect a strong HI absorption line peaking at $\nu_{\text{HI,peak}} = 851.03 \text{ MHz}$ ($z_{\text{HI,peak}} = 0.6687$, see Fig. 1). The HI absorption is only detected against the peak of the continuum, coincident, therefore, with the VLBI-scale structure. The line width is $FWHM = 100 \text{ km s}^{-1}$ and the optical depth $\tau_{\text{peak}} = 0.437$. With these values, assuming a spin temperature of 100 K, we obtain an HI column density of $8.05 \times 10^{21} \text{ cm}^{-2}$. These values are in good agreement with those found by Carilli et al. (1998).

No broad absorption (i.e. with $FWHM > 100 \text{ km s}^{-1}$), with optical depth higher than $\tau_{2\sigma} \sim 0.03$, has been detected.

4.2. The source OQ 208

In the radio source OQ 208 we detect a shallow ($\tau_{\text{peak}} = 0.005$) and very broad ($FWZI \sim 1800 \text{ km s}^{-1}$) HI absorption (Fig. 2a). This absorption extends from ~ 21650 to $\sim 23450 \text{ km s}^{-1}$, therefore mostly blue-shifted compared to the systemic velocity 22957 km s^{-1} from Gallimore et al. (1999). The line profile has a peak located at $\nu_{\text{HI,peak}} = 1318.6 \text{ MHz}$ ($z_{\text{HI,peak}} = 0.0773$). Assuming a T_{spin} of 100 K, we obtain an HI column density of $8.0 \times 10^{20} \text{ cm}^{-2}$.

The HI absorption in OQ 208 was already detected by both Vermeulen et al. (2003) and Morganti et al. (2005) although with different results. Vermeulen et al. (2003) found an HI absorption centered on the same frequency ($\nu = 1318.9 \text{ MHz}$) as in our observations but with a width of 256 km s^{-1} only. The likely

reason for the discrepancy with our results is the fact that the maximum available bandwidth at the WSRT at the time of the survey of Vermeulen et al. (2003) was not large enough to allow the detection of such broad features. More recently, the presence of a broad HI absorption in OQ 208 was reported by Morganti et al. (2005) and interpreted as a fast outflow of neutral hydrogen. Figure 2b shows the comparison between the HI profile derived from the observations presented here and what was found by Morganti et al. (2005). In Fig. 2c, the residuals obtained after subtracting the profiles taken in two different epochs are shown. The figure shows that there is no significant evidence of changes in the HI profile corresponding to an optical depth upper limit of $\tau \sim 0.002$.

It is worth mentioning that the radio source OQ 208 is associated with a broad emission line galaxy at $z = 0.07658$. The radio structure is characterised by two compact lobes, separated by about 10 pc, highly asymmetric in terms of flux density ratio (Stanghellini et al. 1997). In this source, the shape of the radio spectrum could either arise from synchrotron self-absorption or free-free absorption by an external absorber embedding the lobes (Kameno et al. 2000). Furthermore, X-ray observations (Guainazzi et al. 2004) have led to the discovery of a Compton-thick obscured AGN where the column density of the absorber is 10^{21} cm^{-2} . As suggested by Guainazzi et al. (2004), in this source the jets are likely piercing their way through this Compton-thick medium which is pervading the nuclear environment. The outflow detected in HI would be another indication of this process.

4.3. The source J0655+4100

Although no evidence of neutral hydrogen gas has been found in the radio galaxy J0655+4100, an elliptical galaxy at $z = 0.02156$ ($V_{\text{sys}} = 6464 \text{ km s}^{-1}$; Marcha et al. 1996), we find instead, HI in emission in two nearby galaxies. One companion is the spiral galaxy UGC03593 where, centered at 6694 km s^{-1} , $\sim 2 \times 10^9 M_{\odot}$ of HI have been detected. This galaxy is located 65 kpc South-East of J0655+4100. The second companion displays a systemic velocity of 6334 km s^{-1} and is located to the North-West at 55 kpc from the HFP source. In the Digitized Sky Survey (DSS) image it is associated with a faint galaxy for which we find an HI mass of $\sim 2 \times 10^8 M_{\odot}$. This galaxy has not been previously catalogued¹. The two galaxies form a physical compact group with J0655+4100 (Fig. 3) supporting the idea that young radio sources reside in groups, as suggested by other works (Stanghellini et al. 1993), based on the excess of galaxy density in the optical images of GPS radio sources.

5. Discussion

The detection in HI absorption of only two of the six observed galaxies is somewhat surprising. Analysing a sample of 41 CSS/GPS radio sources, Pihlström et al. (2003) have found an inverse correlation between the source linear size and the HI column density: smaller sources ($< 0.5 \text{ kpc}$) have larger HI column density than the larger sources ($> 0.5 \text{ kpc}$). Following this correlation, one would have expected very high N_{HI} in the smallest sources, like HFPs.

In Fig. 4 we show the inverse correlation found by Pihlström et al. (2003) with the addition of the values obtained from the sources presented in this paper. The sensitivity reached by the

¹ Based on results from the NASA/IPAC Extragalactic Database (NED).

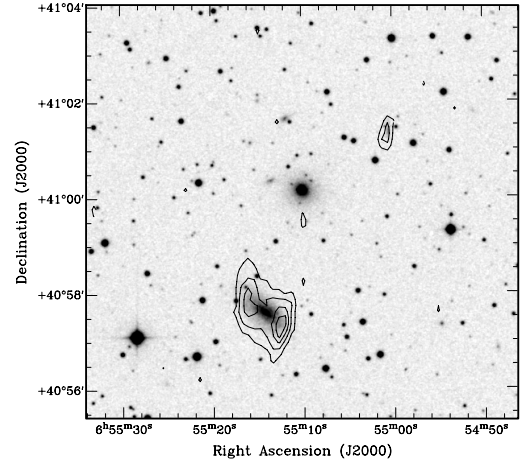


Fig. 3. HI total intensity contours superimposed onto a DSS optical image centered on the radio galaxy J0655+4100. Two nearby galaxies are clearly detected. Contours levels are: $2.35, 3.50, 5.68$ and $7.51 \times 10^{20} \text{ atoms cm}^{-2}$.

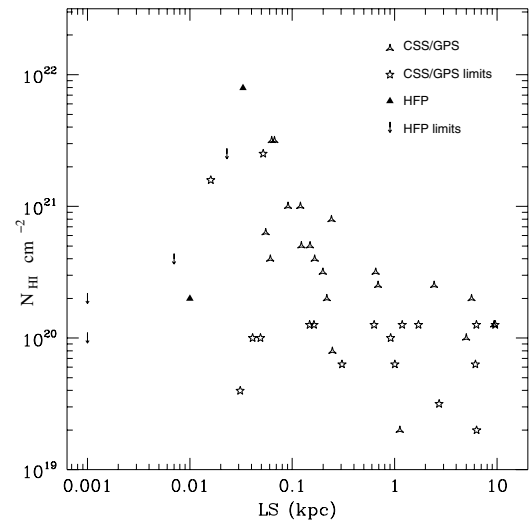


Fig. 4. Absorbed HI column density versus projected linear sizes. The HFP galaxies do not seem to follow the trend found for CSS/GPS sources. The CSS/GPS values have been taken from Pihlström et al. (2003).

new observations, enables us to set tight upper limits to the N_{HI} for the sources with no HI detection. Interestingly, in our sample, the smallest sources (with size $\lesssim 10 \text{ pc}$) appear to deviate from the extrapolation of the trend found by Pihlström et al. (2003). Given the limited number of objects, we cannot establish whether for very compact radio sources a break down of the correlation occurs. If we consider that 15 out of 41 sources of Pihlström et al. (2003) sample have HI column density below $2 \times 10^{20} \text{ cm}^{-2}$, the probability to find two sources randomly chosen both below such limit is $\sim 13\%$. This means that the small column density is possibly a feature typical of extremely young radio galaxies. We also point out that the correlation from Pihlström et al. (2003) has a large scatter, and upper limits to the column density are present at all linear sizes. With all this in mind, it is interesting to consider the possible origin of the lack of HI absorption found in J0655+4100 and J1623+5524.

The trend observed by Pihlström et al. (2003) has been explained with both a spherical and axi-symmetric gas distribution, with a radial power law density profile, as well as a disk

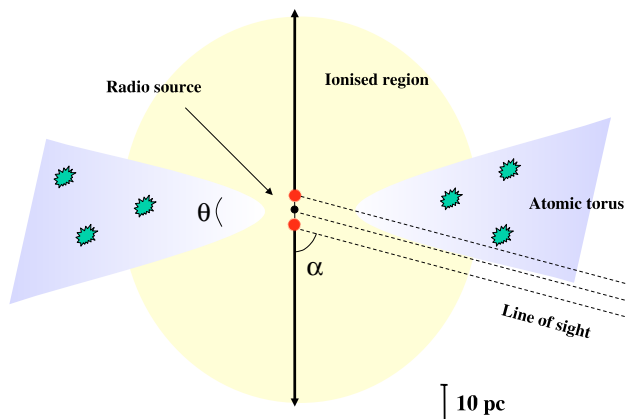


Fig. 5. Cartoon of a possible orientation of the HFP sources and circumnuclear torus. The toroidal structure is perpendicular to the source axis. The torus model is dependent on the opening angle θ and the viewing angle α . The scale shown is approximate: the inner radius of the torus and the sizes of the denser clumps are not known.

model. Indeed, a torus-like distribution of neutral gas has been found to be consistent with the observations in a number of GPS sources (i.e. 4C 31.04 by Conway 1996; 1946+708 by Peck et al. 1999). In this scenario, the absence of high HI column density in very compact sources can be explained by both the orientation and the extreme compactness of the sources. Within the framework of the AGN unification scheme, the central engine is surrounded by a disk of ionised gas and shielded by an obscuring torus of atomic and molecular gas (i.e. Urry & Padovani 1995). Evidence of ionised disks with radii between a few tens and one hundred pc has been claimed in this class of sources (Kameno et al. 2000), as responsible of free-free absorption in the optically thick region of the radio spectrum.

The fundamental ingredient to trace HI absorption is the presence of background flux density. Given the extremely small linear sizes of the HFP sources (see Fig. 4 and Table 1), the line of sight likely passes mainly through the ionised region, piercing the torus only in its very inner part, if we are looking at the receding lobe. This could be the case if the torus axis is aligned to the radio jet, and its half-opening angle is, for example, $\theta \sim 20^\circ$ (as illustrated in Fig. 5), consistent with the constraint $\theta \leq 30^\circ - 40^\circ$ by Granato et al. (1997), and an orientation of the line of sight between 45° and 70° (with respect to the radio jet).

It should be noted that the gas closer to central engine is hotter, both in terms of kinetic and spin temperature, therefore a longer path length would not necessarily imply a higher optical depth. Moreover, recent work by Hatziminaoglou et al. (2006) focused on the properties of the dusty tori in AGN, has shown the possibility of low optical depth tori. Therefore, in this scenario, it is possible that for these sources of a few pc in size (or even less), we are missing the HI absorption due to both sensitivity limitations and orientation effects.

As described in Sect. 1, in addition to the presence of circumnuclear tori, in such young radio sources one could have expected to detect also the presence of unsettled gas, i.e. gas not necessarily located in a circumnuclear torus or disk-like structure but still enshrouding the radio source. We do not find evidence for this. Again, this could be partly due to the very small emitting area of the background radio source, that decreases the probability to detect the absorption. Clouds indicating the presence of a rich and clumpy interstellar medium in the centre of the radio source have been found as in the case of 4C 12.50 (Morganti et al. 2004b), 3C 49 and 3C 286.3

(Labiano et al. 2006). In 4C 12.50 a cloud of $\sim 20 \times 60$ pc has been detected: such a cloud would have covered most of the HFPs in our sample. Thus, our results are possibly indicating that the filling factor of such clouds is low, as it could be the case in 4C 12.50.

Finally, the great majority of the fast outflows detected in both pc- and kpc-scale radio galaxies have an HI optical depth of only $\tau < 0.006$ (Morganti et al. 2005). Our observations are not sensitive enough to reach such low values, therefore the lack of detection of broad absorption (except for the case of OQ 208 where the continuum is indeed strong enough) indicates that HI outflows are characterized by low optical depths.

6. Conclusions

An HI absorption search has been carried out with the WSRT for a sample of 6 HFP radio galaxies. We confirm the detection of HI in absorption in 2 galaxies. One source, J0111+3906, is characterised by a line width of $\sim 100 \text{ km s}^{-1}$ and a high optical depth of $\tau = 0.44$. In the other source (OQ 208), the line profile is very broad ($\sim 1800 \text{ km s}^{-1}$), blue-shifted and shallow, with a maximum optical depth of $\tau = 0.005$. In the remaining 4 galaxies no evidence of HI absorption has been detected.

Although this result does not seem to follow the inverse correlation found (Pihlström et al. 2003) between the column density and the linear sizes, it can be explained by orientation effects in a torus scenario, in which our line of sight intersects the torus in its inner region where the low optical depth is due to high spin and kinetic temperature. Since these 4 sources have faint flux densities, optical depths ≤ 0.01 are not detectable due to sensitivity limitations. Therefore, the HI absorption in an object with the same spectral characteristics of OQ 208 but with a fainter flux density, cannot be detected by our observations.

Although HFP sources do not seem to follow the correlation between HI column density and linear size found for CSS/GPS sources, this does not imply that we are looking at a different class of objects, instead of the youngest tail of a radio source population. Our results suggest that on linear scales smaller than few tens of parsecs, the HI column density is much lower than one would have expected on the basis of the work of Pihlström et al. (2003). As a consequence, compact and rather faint (due to self-absorption) sources, such as these HFPs, are not the most suitable class of objects to investigate the HI absorption on such a small scale.

Acknowledgements. We are grateful to T.A. Oosterloo for helpful suggestions on the best use of the software MIRIAD. MO acknowledges the Kapteyn Astronomical Institute of the University of Groningen and ASTRON for their hospitality during this project. Part of this research was funded by RadioNet and the Nova-Marie Curie Fellowship programme. We thank the referee, René Vermeulen, for useful comments which improved the paper. The WSRT is operated by ASTRON (The Netherlands Foundation for Research in Astronomy) with support from the Netherlands Foundation for Scientific Research (NWO). This research has made use of the NASA/IPAC Extragalactic Database (NED), which is operated by the Jet Propulsion Laboratory, California Institute of Technology, under contract with the National Aeronautics and Space Administration.

References

- Baum, S. A., O’Dea, C. P., de Bruyn, A. G., et al. 1990, *A&A*, 232, 19
- Carilli, C. L., Menten, K. M., Reid, M. J., et al. 1998, *ApJ*, 494, 175
- Conway, J. E. 1996, *IAUS*, 175, 92
- Conway, J. E. 1999, *NewAR*, 43, 509
- Conway, J. E., & Blanco, P. R. 1995, *ApJ*, 449, 131
- Dallacasa, D. 2003, *PASA*, 20, 79

- Dallacasa, D., Fanti, C., Fanti, R., Schilizzi, R. T., & Spencer, R. E. 1995, *A&A*, 295, 27
- Dallacasa, D., Stanghellini, C., Centonza, M., & Fanti, R. 2000, *A&A*, 363, 887
- Dallacasa, D., Falomo, R., & Stanghellini, C. 2002, *A&A*, 382, 53
- Fanti, R., Fanti, C., Schilizzi, R. T., et al. 1990, *A&A*, 231, 333
- Fanti, C., Fanti, R., Dallacasa, D., et al. 1995, *A&A*, 302, 317
- Gallimore, J. F., Baum, S. A., O'Dea, C. P., Pedlar, A., & Brinks, E. 1999, *ApJ*, 524, 684
- Granato, G. L., Danese, L., & Franceschini, A. 1997, *ApJ*, 486, 147
- Guainazzi, M., Siemeginowska, A., Rodriguez-Pascal, P., & Stanghellini, C. 2004, *A&A*, 421, 461
- Hatziminaoglou, E., et al. 2006, *ASP Conf. Ser.* [[arXiv:astro-ph/0603359](https://arxiv.org/abs/astro-ph/0603359)]
- Heckman, T. M., Balick, B., van Breugel, W. J. W., & Miley, G. K. 1983, *AJ*, 88, 583
- Kameno, S., Horiuchi, S., Shen, Z.-Q., et al. 2000, *PASJ*, 52, 209
- Labiano, A., Vermeulen, R. C., Barthel, P. D., et al. 2006, *A&A*, 447, 481
- Marcha, M. J. M., Browne, I. W. A., Impey, C. D., & Smith, P. S. 1996, *MNRAS*, 281, 425
- Morganti, R., Oosterloo, T. A., Tadhunter, C. N., et al. 2001, *MNRAS*, 323, 331
- Morganti, R., Oosterloo, T., Tadhunter, C. N., et al. 2004a, *A&A*, 424, 119
- Morganti, R., Greenhill, L. J., Peck, A. B., Jones, D. L., & Henkel, C. 2004b, *NewAR*, 48, 1195
- Morganti, R., Tadhunter, C. N., & Oosterloo, T. A. 2005, *A&A*, 444, 9
- Murgia, M. 2003, *PASA*, 20, 19
- O'Dea, C. P. 1998, *PASP*, 110, 493
- Orienti, M., Dallacasa, D., Tinti, S., & Stanghellini, C. 2006, *A&A*, 450, 959
- Owsianik, I., Conway, J. E., & Polatidis, A. G. 1998, *A&A*, 336, 37
- Peck, A. B., Taylor, G. B., & Conway, J. E. 1999, *ApJ*, 521, 103
- Pihlström, Y. M., Conway, J. E., & Vermeulen, R. C. 2003, *A&A*, 404, 871
- Polatidis, A. G., & Conway, J. E. 2003, *PASA*, 20, 69
- Readhead, A. C. S., Taylor, G. B., Xu, W., et al. 1996, *ApJ*, 460, 612
- Snellen, I. A. G., Schilizzi, R. T., Miley, G. K., et al. 2000, *MNRAS*, 319, 445
- Stanghellini, C., O'Dea, C. P., Baum, S. A., & Laurikainen, E. 1993, *ApJS*, 88, 1
- Stanghellini, C., Bondi, M., Dallacasa, D., et al. 1997, *A&A*, 318, 376
- Stanghellini, C., O'Dea, C. P., Dallacasa, D., et al. 2005, *A&A*, 443, 891
- Taylor, G. B., Readhead, A. C. S., & Pearson, T. J. 1996, *ApJ*, 463, 95
- Tinti, S., Dallacasa, D., de Zotti, G., Celotti, A., & Stanghellini, C. 2005, *A&A*, 432, 31
- Urry, C. M., & Padovani, P. 1995, *PASP*, 107, 803
- van Gorkom, J. H., Knapp, G. R., Ekers, R. D., et al. 1989, *AJ*, 97, 708
- Vermeulen, R. C., Pihlström, Y. M., Tschager, W., et al. 2003, *A&A*, 404, 861